

Biodegradable Polyimidazole Particles as Contrast Agents produced by Direct Arylation Polymerization

Felicitas Jansen^{1,2}, Philipp Schuster¹, Markus Lamla¹, Christian Trautwein³ and Alexander J. C. Kuehne^{1,2}*

- 1: Institute of Organic and Macromolecular Chemistry, Ulm University, Albert-Einstein-Allee 11, 89081 Ulm, Germany.
- 2: DWI – Leibniz Institute for Interactive Materials, Forckenbeckstraße 50, 52076 Aachen, Germany.
- 3: Department of Internal Medicine III, University Hospital RWTH Aachen, Pauwelstraße 30, 52074 Aachen, Germany.

ABSTRACT

Conjugated polymer particles provide an important platform for the development of theranostic nanoagents. However, the number of biocompatible and foremost biodegradable π -conjugated polymers is limited. Imidazole is a π -conjugated motif that is abundant in biological systems. Oxidative degradation of imidazole is present in nature *via* enzymatic or free radical processes. In this work, we introduce polymer particles consisting purely of polyimidazole. We employ direct arylation polymerization and adapt it to a dispersion polymerization protocol to yield uniform and narrowly dispersed nanoparticles. We employ this mechanism to produce linear and crosslinked

polymer particles to tune the optical properties from fluorescent to photoacoustically active. We show that the particles can be degraded by H₂O₂ as well as by reactive oxygen species produced by cells and we detect the degradation products. Altogether our results suggest that polyimidazole particles represent ideal candidates for theranostic applications.

INTRODUCTION

Nanomedicine plays a significant role in the diagnosis, monitoring and treatment of many diseases.^{1,2} Conjugated polymer nanoparticles have shown great potential as contrast agents in fluorescence and photoacoustic imaging.^{3–6} Compared to small molecular contrast agents nanoparticles are advantageous in their high fluorescence and photostability.^{7–9} In addition to their outstanding optical properties, nanoparticles of conjugated polymers can be used for passive targeting, where they make use of the enhanced permeation and retention (EPR) effect. Alternatively, they can be transformed to theranostic nanoparticles by surface functionalization so that specific biomolecular targeting motifs can be attached, allowing site specific staining for contrast as well as for drug release.^{10,11} Dispersion polymerization is one means to obtain conjugated polymer nanoparticles of low dispersity.^{12–14} This polymerization technique allows precise adjustment of the particle size in the range of about 100 nm and up to the micrometer scale under mild reaction conditions.^{14–16} A variety of transition metal based C-C cross-coupling reactions like Suzuki, Heck, and Sonogashira-coupling have been employed in dispersion polymerization protocols yielding uniform and monodisperse particles.^{14–16} However, the monomers for these coupling reactions need to be equipped with specific functional groups to take part in the catalytic cycle. By contrast, direct C-H arylation offers a more atom economic alternative, especially to Suzuki-coupling.^{17–20} The direct arylation approach has already been

applied to the synthesis of conjugated polymers;²¹ however, it has not yet been adapted to the dispersion polymerization protocol to synthesize narrowly dispersed or uniform conjugated polymer particles.

A prerequisite for the application of polymer nanoparticles in biomedical applications is that they can be degraded into units that are smaller than the critical diameter of 5-6 nm for renal clearance.^{22–24} Particles and entities larger than that would accumulate in the body, which in turn could lead to toxic effects in the short or long term.^{25–27} To use nanoparticles safely, polymers that make up the nanoparticles must be degradable *via* biologically available processes in the body. Imidazole represents a conjugated unit, which has been shown to be degradable by exposure to reactive oxygen species (ROS). ROS are produced by macrophages in the body.^{28,29} The imidazole motif is common in biological systems, for example it features in the amino acid histidine and occurs in a variety of luminescent biomolecules, such as in the emitter unit of the green fluorescent protein. As a result, imidazole-derivatives have been investigated for biomedical applications.³⁰ A previous attempt to synthesize a homopolymer with the imidazole in the conjugated backbone has been achieved by coupling a dibromo bisimidazole by Yamamoto cross-coupling.³¹ The resulting polymer displayed absorption in the visible spectrum, making it a potential candidate for optical biomedical imaging techniques. However, Yamamoto coupling requires stoichiometric amounts of nickel catalyst, which entails extensive purification of the obtained polymer and the residual traces of heavy metal Ni precludes biological applicability. The resulting polyimidazole is only soluble in organic solvents further complicating application of these polyimidazoles as contrast agents.

Direct arylation polymerization (DAP) of imidazole into particles would circumvent the described problems, because catalyst load could be reduced and particles can be rendered colloidally stable

using biocompatible dispersing agents, enabling application of polyimidazole particles in aqueous biological systems. Such polyimidazole particles could be used as contrast agents or as vehicles for drug delivery as the imidazole motif can be degraded. However, the lack of a suitable polymerization method obviates the availability of such biocompatible polyimidazole particles.

In this work, we develop a DAP protocol for the dispersion polymerization technique synthesize uniform polyimidazole particles. We show that the particle diameter can be adjusted precisely from below 100 nm up to several hundred nanometers. We characterize the optical properties of the obtained particles and investigate their degradation mechanism and the biocompatibility of these units.

RESULTS AND DISCUSSION

The key to develop DAP for imidazoles and adapt it to a dispersion polymerization approach, is to use a palladium catalyst with adamantylphosphine oxide ligands. Other typical ligands such as pivalic acid fail to produce particles. The palladium catalyst with adamantylphosphine oxide ligands has previously been used to couple structurally related oxazolines and indoles.^{19,32} To obtain particles of linear polymer chains we utilize 5-iodo-1,4-dimethylimidazole as a monomer (**P1** in Figure 1a). When leaving the 4-position of the imidazole unblocked, we obtain a crosslinked imidazole polymer network **P2** (see Figure 1a).³³

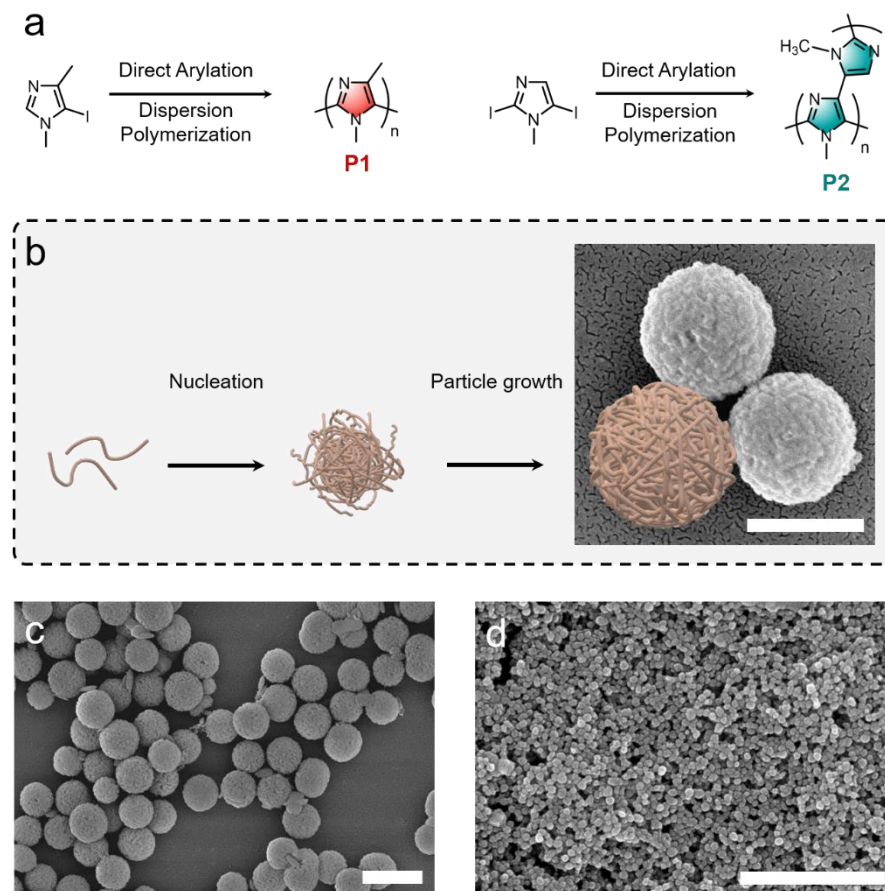
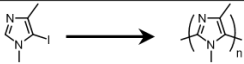
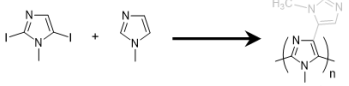
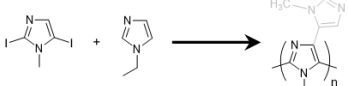
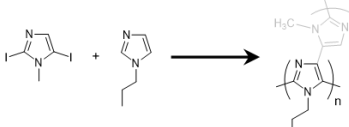

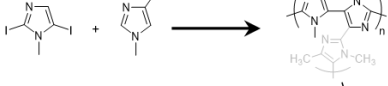
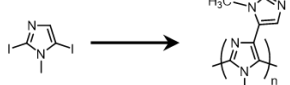


Figure 1. Direct arylation polymerization to synthesize polyimidazole particles. (a) Reaction scheme for the synthesis of linear polymer particles P1 (red) and crosslinked polymer particles P2 (cyan). (b) Schematic illustration of a dispersion polymerization, including a SEM image of P1 particles. The scale bar represents 500 nm. (c) SEM image showing P1 particles, with an average size of 572 ± 43 nm. The scale bar represents 1 μm . (d) SEM image showing P2 particles, with an average size of 38 ± 8 nm. The scale bar represents 1 μm .

DAP of the imidazole monomers in the presence of stabilizers and in a solvent that is good for the monomers but bad for the polymer yields particles (Figure 1b).^{16,34,35} In the beginning of a dispersion polymerization, all reactants are dissolved. This includes catalyst, monomers, as well as stabilizers and base. When reaching the critical molar mass for solubility of the polymer, nucleation occurs and further DAP yields chains that condensate onto these nuclei enabling growth of the particles. Here, we use *n*-propanol as a suitable solvent and potassium *tert*-butoxide as base. The stabilizing agents are poly(vinylpyrrolidone-*co*-vinyl acetate) (PVPVA) and Triton X-45 (non-ionic surfactant), which prevent aggregation and provide colloidal stability to the particles.

The obtained particles are purified by consecutive centrifugation and redispersion in *n*-propanol or water to remove byproducts, unreacted monomers, and excess stabilizers (see Experimental Methods). We analyze the purified particles using scanning electron microscopy (SEM) revealing that the choice of monomer has a strong effect on the size of the particles. While we obtain particles with an average diameter (d) of around 570 nm for **P1**, we obtain much smaller particles with $d < 50$ nm for **P2** using the same reaction conditions (Figure 1c and Figure 1d). We extend our study by applying different imidazole monomers and analyzing the resulting particles (Table 1, and Table S1). The reaction conditions established for **P1** and **P2** are precisely transferrable to other types of imidazole monomers. Introduction of an ethyl or propyl residue to the 1-N position does not have a significant impact on the size and shape of the particles. By contrast, increasing of the probability for crosslinking results in decreasing particle diameters as well as reduced absorption wavelength λ_{abs} (see Table 1). The absorption wavelength is a function of the conjugation length of a conjugated polymers, allowing us to hypothesize that particles with shorter λ_{abs} exhibit shorter conjugation lengths and are therefore more strongly branched or crosslinked. Indeed, only **P1** particles can be dissolved in DMF as a good solvent for the polymer, whereas all other particles only swell and maintain their globular particle shape, as their molecular structure will exhibit some degree of branching or crosslinking. More crosslinked particles exhibit also reduced uniformity, which can be understood by recognizing that in linear chains the critical molar mass is approached in a more controlled way as compared to monomers that can branch or crosslink (see Table 1).

Table 1. Overview of all different monomers used to synthesize polymer particles with the respective size and maximal absorbance wavelength.

	Reaction	d (@ $[M] = 116 \text{ mM}$) (nm)	λ_{abs} (nm)
P1		572 ± 43	431
P1a		308 ± 33	275
P1b		396 ± 64	398
P1c		273 ± 84	392
P1d		209 ± 47	277
P1e		77 ± 18	256
P2		38 ± 8	scattering

For biomedical *in vivo* applications, it is essential that the particles do not exceed $d = 400 \text{ nm}$ as larger particles will be receptive to the EPR effect, which enables some degree of targeting also in the absence of molecular recognition motifs.³⁶ Therefore, we conduct a concentration study on **P1a** particles to showcase that precise adjustment of d is possible, with diameters as small as 50 nm and up to about 350 nm (see Figure 2a,b).

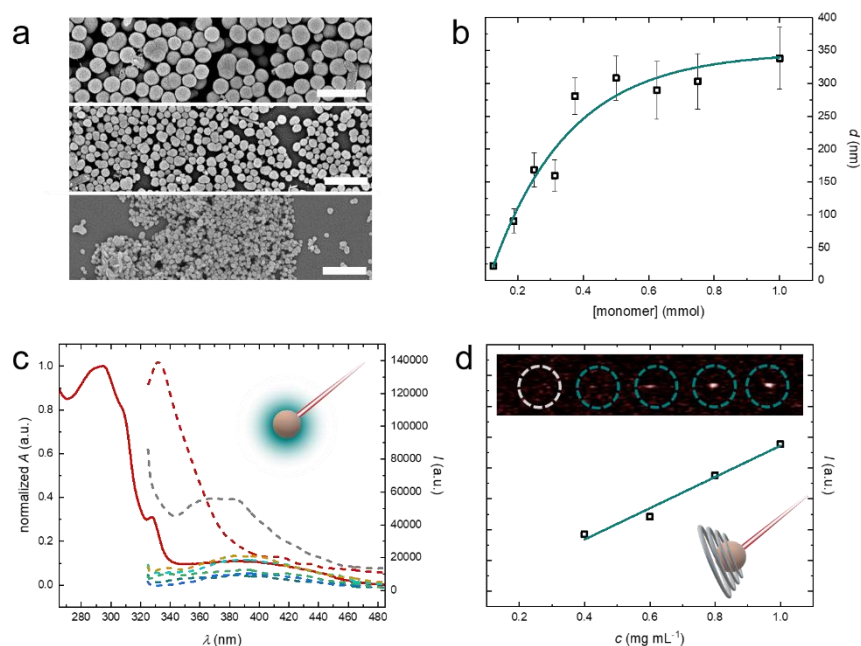


Figure 2. Characterization of the synthesized polymer particles. (a) Overview of particles **P1a** with three different sizes. All scale bars represent 1 μm . (b) Size adjustment of the particles **P1a** by varying the monomer concentration. The error bars indicate the uniformity of the particles. (c) Optical characterization of the polymer particles. The red continuous line shows the absorption spectrum of linear polyimidazole polymers synthesized in solution. The dashed lines indicate the fluorescence of the particles when being excited at 300 nm (**P1**-red; **P1a**-blue; **P1b**-grey; **P1c**-green; **P1d**-orange; **P1e**-light blue; **P2**-cyan). To compare the intensity of the particles, all spectra are recorded at a concentration of 0.2 mg/mL in 1-propanol. Whereas **P1** exhibits a strong fluorescence, the intensity of all other particles is comparatively small. The inset shows a schematic representation of a fluorescent particle. (d) Photoacoustic behavior of **P2**. There is a linear dependency between the photoacoustic intensity and the used particle concentration. The inset at the top represents the photoacoustic response of the corresponding particle concentration (from red=low to white=high intensity). All measurements are performed in water using an LED at 850 nm. The small inset in the bottom right corner illustrates a photoacoustically active particle.

The UV/Vis absorbance spectra of small polyimidazole particles are strongly dominated by scattering, especially for particles with $d < 200$ nm. To obtain information about the absorption resulting from the conjugated nature of the molecular backbone, we take the UV/Vis absorption spectrum of a linear polyimidazole polymer synthesized in solution as a reference (see Experimental Methods). The solution of the linear polyimidazole exhibits strong absorption at 300 nm. Next, we excite our particles at this wavelength and record the fluorescence to evaluate

whether the particles are suitable for fluorescence imaging. We prepare dispersions of particles in 1-propanol with a concentration of 0.2 mg/mL. **P1** exhibits much stronger fluorescence compared to all other particles (see Figure 2c). As fluorescence is a feature of the molecular structure, we hypothesize that branching in the 4-position of the imidazole repeat unit is detrimental to fluorescence and will probably feature non-radiative relaxation of the excited state. **P2** only shows a very weak fluorescence, and we therefore expect that non-radiative relaxation will take place *via* vibronic pathways, which could allow us to follow the particles by photoacoustic imaging rather than fluorescence. Here, vibronic relaxation of a photoexcited state is recorded by the produced ultrasound waves that are generated upon pulsed excitation.³⁷

For our **P2** particles, we observe a strong photoacoustic signal for wavelengths between 820 nm and 940 nm (see Figure 2d and Figure S2). The relationship between concentration and photoacoustic signal is linear, which is consistent with the literature on photoacoustic active particles.³⁶ We can detect photoacoustic signal for low intensity excitation (850 nm; 200 μ J/pulse) down to concentrations of 400 μ g/mL (see Figure 2d). The possibility to use these excitation wavelengths in the near infrared (NIR) spectrum enables application of the particles as contrast agents *in vivo*, as NIR can penetrate through tissue much deeper than visible or UV light. The photoacoustic activity supports our hypothesis that non-radiative relaxation is the preferential pathway in crosslinked polyimidazole particles instead of fluorescence.

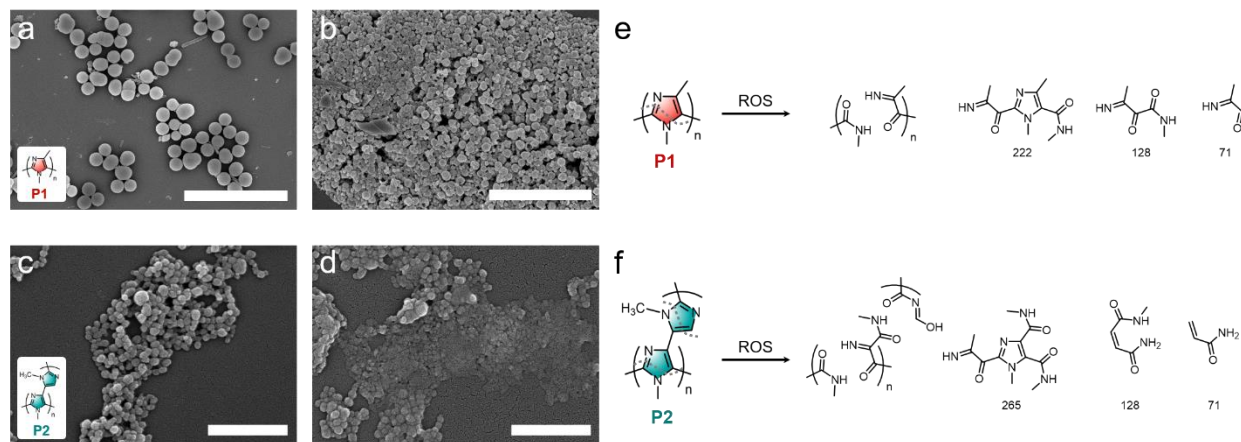


Figure 3. Particle degradation by applying H_2O_2 as reactive oxygen species. (a) SEM image of **P1** before degradation. (b) SEM image of the **P1** particle dispersion after H_2O_2 exposure for 24 h. (c) and (d) SEM images of **P2** before and after degradation by exposure to H_2O_2 for 24 h. The scale bars in (a) and (b) represent 5 μm in (c) and (d) 500 nm. (e) and (f) show the proposed degradation of linear **P1** and crosslinked **P2** particles alongside a series of representative fragmented degradation products (see Supporting Information for more details).

Being present in so many functional biological units, imidazoles can be degraded by enzymatic oxidation.²⁸ It has also been described that hydrogen peroxide and ROS produced by macrophages can cleave and degrade the imidazole units.^{29,38} To test whether our particles could also be degraded by macrophages, we first perform a simplified degradation procedure by exposing an aqueous dispersion of particles to hydrogen peroxide. We monitor the particles over the course of 24 h using UV/Vis spectroscopy and we take aliquots for analysis by SEM (see Figure 3a-d and Figure S3). For the **P1** particles, we observe a significant decrease in size after 24 h. From the initial size of 570 nm, the uniformity as well as the diameter decreases after 24 h of degradation, resulting in a broad distribution of particle sizes with diameters below 100 nm (see Figure 3a,b). Such high dispersity indicates uncontrolled degradation and corrosion of the particles from the outside. UV/Vis spectroscopy provides a gradually decreasing absorbance for advancing degradation (see Figure S3a). For **P2** particles, we observe a similar trend of decreasing absorbance, while monitoring of the reduction in diameter is not as easy as **P2** particles are much

smaller from the start (see Figure 3c,d and Figure S3b). To obtain information about the degradation products we apply chemical ionization mass spectrometry (CI-MS). The obtained mass spectra of the degradation products show groups of peaks separated by a mass of 1 indicating that there is a mixture of degradation products where N and O can be interchanged as a consequence of the oxidative degradation process. Furthermore, there is a superordinate spreading with a separation representing the weight of an imidazole unit. The larger separation will be the effect of incomplete degradation and the presence of degraded oligomers. The CI-MS analysis allows us to identify a selection of the most frequent degradation products in agreement with the oxidative degradation mechanism (see Figure 3e,f). We conclude that in contrast to the enzymatic degradation of imidazole, where a distinct degradation products have been presented,^{28,39} hydrogen peroxide induced degradation is much less controlled and results in a greater variety of degradation products (see Figure 3e,f and Figure S4 and S5).

To display that our particles can also be degraded at concentrations produced by cells, while at the same time being powerful contrast agents, we employ **P1** particles as fluorescent nanoparticles for imaging of J774 A.1 macrophage cells. To prove that J774 A.1 macrophages take up our **P1** particles, we stain the cells with a suitable UV dye (CellTracker™ Blue CMHC) culture them in FluoroBrite™ medium and expose them to a **P1** particle dispersion in phosphate buffered saline (PBS). We analyze the uptake process straight after addition of the **P1** particles by confocal microscopy. We excite the **P1** particles at 633 nm to avoid crosstalk with the CellTracker™ dye and to avoid autofluorescence of the macrophages. In the beginning, we observe free particles, which become internalized by the cells within 1 h of incubation (see Figure 4a-c).

To activate ROS production in the J774 A.1 macrophages, we stimulate the cells with lipopolysaccharide (LPS), a well-established reagent and process for the activation of

macrophages.^{29,40} After incubating the macrophages with particles for 3 h, we again make use of confocal microscopy to monitor the degradation process. We identify cells that have taken up several nanoparticles, which we image again 4 h later (7 h after activation). To make sure we do not miss particles by recoding a slice through the cell that does not contain particles, we record z-stacks to image the identified cells in 3D (see Supplementary Videos). The fluorescence of the particles has decreased significantly and completely disappears after 2 more hours, leading to the conclusion that particle degradation by activated macrophages is possible within the timeframe of 9 h (Figure 4f and Figure 4g). We can exclude that the decrease in fluorescence is caused by photobleaching, because the particles have also disappeared in the bright-field images. Moreover, we see free fluorescent particles in the cell medium that have not been taken up by macrophages. These particles are exposed to the same amount of light as the degraded particles inside the cells, allowing us to rule out photobleaching.

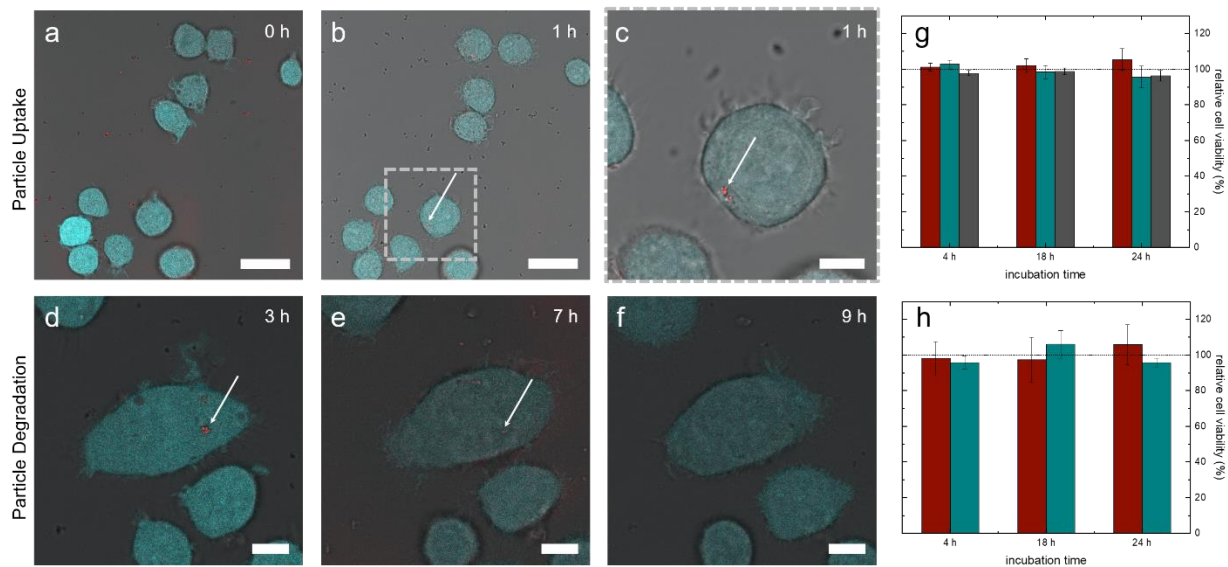


Figure 4. Uptake and degradation in cell culture: Confocal images of (a)-(c) particle uptake and (d)-(f) particles degradation after LPS activation by J774A.1 macrophages. The white arrows indicate the presence of **P1** particles. (a) Confocal image of blue stained macrophages incubated with **P1** particles at $t = 0$ h, (b) same region of interest at $t = 1$ h. (c) Zoom in on the dashed square in (b) displaying a cell that has taken up particles at $t = 1$ h. (d) Confocal image

of LPS activated macrophage with particles $t = 3$ h of incubation. The particles are clearly visible by their red fluorescence. (e) and (f) Same region of interest as in (d) at $t = 7$ h (e) and $t = 9$ h (f). The fluorescence of the particles becomes weaker and disappears indicating complete degradation of the particles. The scale bars in (a) and (b) represents 25 μm ; in (c) to (f) 8 μm . (g) Cell viability of particles **P1** (red) and **P2** (cyan) for J447A.1 cells after 4 h, 18 h, and 24 h of incubation. Exposure of J447A.1 to **P1** together with 1 $\mu\text{g/mL}$ of LPS (for ROS activation) is shown in grey. (h) Cell viability of particles **P1** (red) and **P2** (cyan) exposed to HeLa cells for 4 h, 18 h, and 24 h. All particle concentrations in (g) and (h) are 10 $\mu\text{g/mL}$.

We are also interested, whether the degradation products are toxic to the cells. We could not observe any signs of cytotoxicity during the degradation cell experiments, which is why we repeat uptake and degradation experiments and incubate the J774 A.1 cells of a longer period of time. As a measure for the cell viability, we perform an assay of the ATP level. Neither **P1** nor **P2** particles nor the degrading **P1** particles show cytotoxic effects at concentrations of 10 mg/mL over the course of 24 h (see Figure 4g). To get an impression of how other cell types behave when exposed to our polyimidazole particles, we extend the viability studies to HeLa cells. In a standard MTT assay, with particle concentrations of 10 $\mu\text{g/mL}$ we see low cytotoxicity over 24 h similar to the results with the J774 A.1 cells (see Figure 4h). At higher concentrations of 200 $\mu\text{g/mL}$ the relative viability decreases to 60 % (see Figure S6). We have to note, that these are particle concentrations where the cells are heavily loaded with particles. Therefore, we cannot determine with high confidence whether we have reached a toxic concentration of the degradation products or whether the cells are suffering under the high load of internalized particles.

CONCLUSIONS

In summary, we have developed polyimidazole particles with great potential as contrast and delivery vehicles in the field of biomedicine. Their hydrophobic nature could in the future be used to encapsulate and release hydrophobic drugs. The possibility of tuning the particle diameters to less than 100 nm enables passive targeting strategies (such as the EPR-effect) to enter inflamed or

cancerous tissue. Our particles represent one of the few examples, where degradation and possible release is triggered by ROS. This trigger could play an important role for release and imaging of inflammations or tumors with high oxidative stress. Here, tumor associated macrophages produce high levels of ROS and could trigger degradation once the particles have entered the pathological tissue. In the future, *in vivo* studies about the toxicity of the degradation products would be required to progress the materials further into application.

EXPERIMENTAL METHODS

Chemicals: 1,4-Dimethylimidazole, di(1-adamantyl)phosphine oxide and 5-iodo-1,4-dimethylimidazole are purchased from abcr. 2,5-Diiodo-1-methylimidazole and 1-propylimidazole are obtained from ChemPur. 1-Ethylimidazole is received from Merck. The following chemicals are purchased from Sigma-Aldrich: Potassium tert-butoxide, 1-methylimidazole, 5-iodo-1-methylimidazole palladium(II)-acetate as well as the stabilizers poly(1-vinylpyrrolidone-co-vinyl acetate) (PVPVA: average MW ~ 50,000 Da) and Triton X-45. The solvent n-propanol ($\geq 99,7\%$, AnalaR NORMAPUR® ACS) is received from VWR. All chemicals are applied without any further purification.

General synthetic procedure for the direct arylation polymerization: The stabilizers Triton X-45 (800 mg) and PVPVA (720 mg) are dissolved in 1-propanol (3.3 mL). Potassium tert-butoxide (2.14 mmol, 240 mg) is dissolved in n-propanol (2 mL). The monomers (each monomer 0.5 mmol, 1 mmol in case of one monomer) are mixed with n-propanol (3.3 mL) in a round-bottom flask, which is equipped with a stirrer and a rubber septum. The stabilizer solution is added to the reaction flask and subsequently the pale yellow reaction solution is degassed with argon for 10 minutes. Palladium(II)-acetate (0.025 mmol, 5.6 mg) and di(1-adamantyl)phosphine oxide (0.0125 mmol,

4.0 mg) are combined and added to the reaction solution. The reaction solution is heated to 100 °C. After the base solution is degassed with argon for 2 minutes, it is transferred to the reaction vessel via syringe. The reaction is stirred for 4 – 18 h at 100 °C. For purification, the reaction mixture is cooled to room temperature. The particles are received by centrifugation (9000 rpm, 10 min). After the supernatant is discarded, the particles are redispersed in n-propanol using ultrasonication. This purification procedure is repeated five times to yield the polymer particles.

Synthetic procedure for polymerization in solution (Yamamoto): During the synthesis all chemicals are handled in an oxygen and moisture free environment. 2,5-diiodo-1,4-dimethylimidazole (0.14 mmol; 50 mg) and 2,2'-bipyridine (0.22 mmol; 35 mg) are dissolved in DMF (2.5 mL). This solution is degassed with argon several times. The catalyst Ni(COD)₂ (0.18 mmol; 50 mg) is added and the reaction mixture is stirred at 80 °C over night. After the solvent is removed in vacuum, the brown solid is washed with aqueous ammoniac solution and subsequently centrifuged. The residue is dissolved in a mixture of DMSO and CHCl₃ (20/80) and insoluble parts are separated using a short filtration column. The product is obtained with a M_n of 6700 g/mol (determined by GPC).

Field Emission Scanning Electron Microscopy (FESEM): Field emission scanning electron microscopy (FESEM) is executed with a Hitachi S-5200 Cryo-SEM to analyze the size and the shape of the particles. To prepare the samples a dispersion of polymer particles in n-propanol is deposited on a silicon wafer. After air-drying, the wafers are sputtered with a layer (4-8 nm) of gold. The measurements are performed with acceleration voltages of either 5 kV or 10 kV.

UV/Vis spectroscopy: A Lambda 365 spectrophotometer by Perkin Elmer supplied with UV WinLab as standard software is used to perform UV/Vis analysis. For sample preparation, the

polymer particles are dispersed in water or propanol and placed in a 1 cm quartz glass cuvette. The measurements are performed at a constant scan speed of 600 nm min⁻¹.

Fluorescence spectroscopy: The measurements are performed with a FL6500 fluorescence spectrometer from Perkin Elmer. For sample preparation, the polymer particles are dispersed in n-propanol and placed in a 1 cm quartz glass cuvette.

Photoacoustic Imaging (PAI): Photoacoustic measurements are performed using the LED array light source Photoacoustic Imaging System by Cyberdyne LED with AcousticX as standard software. As light sources, high-density high-power LEDs with different wavelength (750/850 nm and 820/940 nm) and selectable pulse widths of 30 ns up to 150 ns are utilized. The measurements are carried out with the speed of sound (1480 m s⁻¹) specific for water as the surrounding medium.

Mass Spectrometry (MS): CI mass spectrometry was performed on a Thermo Scientific ISQ LT using methane as reagent gas.

Gel permeation chromatography (GPC): The molecular weight of the polymer is determined by gel permeation chromatography (GPC) on a self-assembled device with the following components: auto sampler: Agilent 1100; pump: Dionex P580; column oven: Shimadzu CTO-10A VP and refractive index detector: Waters Corp. Model 2410. Polystyrene is used as a standard and DMF as the eluent.

Microscopic macrophage degradation study:

J774A.1 cells (50000) are seeded overnight in a μ -dish (35 mm, Ibidi) in fluorobrite (Gibco, ThermoFisher) + 10 % FBS (Gibco, Thermofisher) + 4 mM L-Glutamine (Sigma-Aldrich) + 1 mM Pyruvate (Sigma-Aldrich) + 100 units/L penicillin (Sigma-Aldrich) + 0.1 mg/L streptomycin (Sigma-Aldrich). Next day, the cells are stained with a cell tracker CellTracker™

Blue CMHC Dye (Invitrogen™, ThermoFisher). For this, a solution of the dye in serum free medium with a concentration of 25 µg/mL is prepared. After removing the fluorobrite, dye solution (2 mL) is added to the cells for one hour. The dye solution is removed and subsequently the cells are washed and incubated with fresh fluorobrite. Immediately afterwards a LPS solution (1 µL; Sigma Aldrich, Lipopolysaccharides from Escherichia coli 0111:B4) and a PBS (Sigma-Aldrich) particle dispersion (20 µL) is injected to give final concentrations of 1 µg/mL LPS and 25 µg/mL particles. Generally, the particles are sterilized and stored in pure ethanol. For the degradation study, an aliquote is washed three times with PBS and subsequently dispersed in 20 µL PBS which is then injected into the cell medium. It has to be stated, that during the washing procedure a high amount of particles sticks to the plastic sides of the centrifugation tubes (Eppendorf), which is why we assume that the final concentration is lower than 25 µg/mL. The cells are monitored by a Leica DMI8 confocal microscope. We use a cell chamber, which has a constant temperature of 37 °C and a CO₂ rich atmosphere of 5 % and air humidity of 95 % water (gas flow: 0.1 L/min). Two excitation wavelength channels are applied, the stained cells are excited at 405 nm and the particles are excited at 633 nm.

Cell cytotoxicity assay:

To determine the cell viability, the MTT assay and the CellTiter-Glo assay are used. The viability is tested with Hela and J774A.1 cells, which are cultivated in a humidified incubator with 5% CO₂ at 37 °C. For the CellTiter Glo assay, J774A.1 cells are seeded in a density of 7500 cells per well into a white 96 well plate and are grown for 24 hours. To determine the influence of LPS on the cell viability, the cells are treated for one hour with 100 µl DMEM containing LPS (1 µg/ml). Subsequently, the medium is replaced by 100 µl fresh DMEM and the cells are incubated for 24 h. In another control experiment, the cells are incubated for 24 hours with 100 µl DMEM containing

1 µg/ml LPS. To determine the cell viability of the nanoparticles, the cells are treated for 4 h, 18 h and 24 h with 100 µl DMEM containing the nanoparticles in a concentration of 10 µg/ml and 200 µg/ml. In a control experiment, cells are treated for 4 h, 18 h and 24 h with 100 µl DMEM containing the nanoparticles in a concentration of 10 µg/ml and 200 µg/ml and in addition LPS with a concentration of 1 µg/ml is added to each approach. To determine the viability, the medium is replaced with 100 µl fresh DMEM and 100 µl CellTiterGlo reagent (Promega) is added. Then the 96 well plate is placed for three minutes on a shaker and subsequently it is incubated for 10 minutes at room temperature. The luminescence is measured by a PromegaTM GloMax® Navigator microplate reader. For the MTT assay, 7500 HeLa cells are plated in a 96 well plate. After 24 h the medium is replaced by 100 µl of fresh DMEM, containing the nanoparticles in a concentration of 10 µg /ml or 200 µg/ml. After that, the cells are incubated for 4h, 18h and 24h. The supernatant is removed and the cells is washed with 100 µl PBS. Subsequently, 100 µl phenol red-free DMEM and 10 µl MTT solution (5mg/ml in PBS) is added. The cells are incubated at 37 °C for 1 h. The supernatant is removed and the formazan crystals are dissolved by adding 100 µl DMSO. The absorption is determined at 550nm using a Tecan Infinite M1000 microplate reader. All experiments are performed in triplicate and the results are shown as the mean +- standard deviation.

ASSOCIATED CONTENT

Supporting Information.

SEM images and absorbance spectra for all synthesized particles, PAI data for P2 at different wavelength, UV/Vis spectra of the process of particle degradation, mass spectra of the degradation products of P1 and P2, cell cytotoxicity studies on HeLa and J774A.1 cells. Video sequences of z-stacks through the cells for localization of our polyimidazole nanoparticles.

AUTHOR INFORMATION

Corresponding Author

*Alexander J. C. Kuehne *

Institute of Organic and Macromolecular Chemistry, Ulm University, Albert-Einstein-Allee 11,
89081 Ulm, Germany; +49 7315022871; alexander.kuehne@uni-ulm.de

Author Contributions

The project was conceived by A.J.C.K and C.T.. Synthesis was done by F.J., and P.S.; material characterization was done by F.J., mass spectrometry was done by M.L.; cell experiments were done by F.J. and M.L.; All data was analyzed by F.J., M.L., and A.J.C.K. The first draft of the manuscript was written by F.J. and A.J.C.K. All authors gave further input and approval to the final version of the manuscript.

Funding Sources

Deutsche Forschungsgemeinschaft (DFG) RTG 2375 "Tumor-targeted Drug Delivery" grant no 331065168.

Notes

Any additional relevant notes should be placed here.

ACKNOWLEDGMENTS

We thank the German Research Foundation (DFG) in the framework of the Research Training Group 2375 "Tumor-targeted Drug Delivery" grant 331065168. We gratefully thank Philipp Schwarz and Meltem Karakaya for support during particle synthesis.

ABBREVIATIONS

ATP, adenosine triphosphate; CHCl₃, chloroform; CI, chemical ionization; DAP, direct arylation polymerization; DMEM, dulbecco's modified eagle medium; DMF, dimethylformamide; DMSO, dimethylsulfoxide; EPR, enhanced permeation and retention; GPC, gel permeation chromatography; H₂O₂, hydrogen peroxide; KO^tBu, potassium potassium *tert*-butoxide; LED, light emitting device; LPS, lipopolysaccharide; MS, mass spectrometry; MTT, 3-(4,5-dimethylthiazol-2-yl)-2,5-diphenyltetrazolium bromide; Ni(COD)₂, bis(cyclooctadiene)nickel(0); PAI, photoacoustic imaging; PBS, phosphate-buffered saline; PVPVA, poly(vinylpyrrolidone-co-vinyl-acetate); ROS, reactive oxygen species; SEM, scanning electron microscopy; UV, ultraviolet.

REFERENCES

- (1) Wang, Y.; Feng, L.; Wang, S. Conjugated Polymer Nanoparticles for Imaging, Cell Activity Regulation, and Therapy. *Adv. Funct. Mater.* **2019**, 29 (5), 1–20. <https://doi.org/10.1002/adfm.201806818>.
- (2) Koo, H.; Huh, M. S.; Ryu, J. H.; Lee, D.-E.; Sun, I.-C.; Choi, K.; Kim, K.; Kwon, I. C. Nanoprobes for Biomedical Imaging in Living Systems. *Nano Today* **2011**, 6 (2), 204–220. <https://doi.org/10.1016/j.nantod.2011.02.007>.
- (3) Wei, Z.; Xin, F.; Zhang, J.; Wu, M.; Qiu, T.; Lan, Y.; Qiao, S.; Liu, X.; Liu, J. Donor–Acceptor Conjugated Polymer-Based Nanoparticles for Highly Effective Photoacoustic Imaging and Photothermal Therapy in the NIR-II Window. *Chem. Commun.* **2020**, 56, 1093–1096. <https://doi.org/10.1039/c9cc07821e>.
- (4) Piwoński, H.; Li, W.; Wang, Y.; Michinobu, T.; Habuchi, S. Improved Fluorescence and

- Brightness of Near- Infrared and Shortwave Infrared Emitting Polymer Dots for Bioimaging Applications. *ACS Appl. Polym. Mater.* **2020**, 2 (2), 569–577. <https://doi.org/10.1021/acsapm.9b00967>.
- (5) Li, K.; Liu, B. Polymer Encapsulated Conjugated Polymer Nanoparticles for Fluorescence Bioimaging. *J. mater. Chem.* **2012**, 22, 1257–1264. <https://doi.org/10.1039/c1jm14397b>.
 - (6) Liu, J.; Geng, J.; Liao, L.; Thakor, N.; Gao, X.; Liu, B. Polymer Chemistry Conjugated Polymer Nanoparticles for Photoacoustic Vascular Imaging. *Polym. Chem.* **2014**, 5, 2854–2862. <https://doi.org/10.1039/c3py01587d>.
 - (7) Thurn, K. T.; Brown, E. M. B.; Wu, A.; Vogt, S.; Lai, B.; Maser, J.; Paunesku, T.; Woloschak, G. E. Nanoparticles for Applications in Cellular Imaging. *Nanoscale Res Lett* **2007**, 2, 430–441. <https://doi.org/10.1007/s11671-007-9081-5>.
 - (8) Yan, J.; Smith, J. E.; Wang, K.; He, X.; Wang, L.; Tan, W. Dye-Doped Nanoparticles for Bioanalysis. *nanotoday* **2007**, 2 (3), 44–50.
 - (9) Fernando, L. P.; Kandel, P. K.; Yu, J.; McNeill, J.; Ackroyd, P. C.; Christensen, K. A. Mechanism of Cellular Uptake of Highly Fluorescent Conjugated Polymer Nanoparticles. *Biomacromolecules* **2010**, 11, 2675–2682.
 - (10) Hild, W. A.; Breunig, M.; Goepferich, A. Quantum Dots – Nano-Sized Probes for the Exploration of Cellular and Intracellular Targeting. *Eur. J. Pharm. Biopharm.* **2008**, 68, 153–168. <https://doi.org/10.1016/j.ejpb.2007.06.009>.
 - (11) Kumar, R.; Roy, I.; Ohulchanskyy, T. Y.; Goswami, L. N.; Bonoiu, A. C.; Bergey, E. J.;

- Tramposch, K. M.; Maitra, A.; Prasad, P. N. Covalently Dye-Linked, Surface-Controlled, and Bioconjugated Organically Modified Silica Nanoparticles as Targeted Probes for Optical Imaging. *ACS Nano* **2008**, 2 (3), 449–456.
- (12) Song, J.; Tronc, F.; Winnik, M. A. Two-Stage Dispersion Polymerization toward Monodisperse , Controlled Micrometer-Sized Copolymer Particles. *J. Am. Chem. Soc.* **2004**, 126, 6562–6563.
- (13) Lok, K. P.; Ober, C. K. Particle Size Control in Dispersion Polymerization of Polystyrene. **1985**, 63, 209–216.
- (14) Kuehne, A. J. C.; Gather, M. C.; Sprakel, J. Monodisperse Conjugated Polymer Particles by Suzuki – Miyaura Dispersion Polymerization. *Nat. Commun.* **2012**, 3, 1087–1088. <https://doi.org/10.1038/ncomms2085>.
- (15) Anwar, N.; Rix, A.; Lederle, W.; Kuehne, A. J. C. RGD-Decorated Conjugated Polymer Particles as Fluorescent Biomedical Probes Prepared by Sonogashira Dispersion Polymerization. *Chem. Commun.* **2015**, 51, 9358–9361. <https://doi.org/10.1039/C4CC10092A>.
- (16) Ciftci, S.; Kuehne, A. J. C. Monodisperse Conjugated Polymer Particles via Heck Coupling—A Kinetic Study to Unravel Particle Formation in Step-Growth Dispersion Polymerization. *Macromolecules* **2015**, 48 (22), 8389–8393. <https://doi.org/10.1021/acs.macromol.5b01932>.
- (17) Chen, F.; Huang, F.; Yao, X.; Li, T.; Liu, F. ORGANIC CHEMISTRY FRONTIERS Direct C – H Heteroarylation by an Acenaphthyl- Based α -Diimine Palladium Complex :

Improvement of the Reaction Efficiency for Bi (Hetero) Aryls under Aerobic Conditions

†. *Org. Chem. Front.* **2017**, 4, 2336–2342. <https://doi.org/10.1039/c7qo00562h>.

- (18) Mercier, L. G.; Leclerc, M. Direct (Hetero) Arylation : A New Tool for Polymer Chemists. **2013**, 46 (7), 1597–1605.
- (19) Ghorai, D.; Keil, H.; Stalke, D.; Zanoni, G.; Tkachenko, B. A.; Schreiner, P. R. Secondary Phosphine Oxide Preligands for Palladium-Catalyzed C – H (Hetero) Arylations : Efficient Access to Pybox Ligands. *Adv. Synth. Catal.* **2017**, 359, 3137–3141. <https://doi.org/10.1002/adsc.201700663>.
- (20) Adamczak, D.; Perinot, A.; Komber, H.; Illy, A.; Hultmark, S.; Passarella, B.; Tan, W. L.; Hutsch, S.; Becker-Koch, D.; Rapley, C.; et al. Influence of Synthetic Pathway, Molecular Weight and Side Chains on Properties of Indacenodithiophene-Benzothiadiazole Copolymers Made by Direct Arylation Polycondensation. *J. Mater. Chem. C* **2021**, 9, 4597–4606. <https://doi.org/10.1039/d1tc00043h>.
- (21) Leclerc, M.; Brassard, S.; Beaupré, S. Direct (Hetero)Arylation Polymerization: Toward Defect-Free Conjugated Polymers. *Polym. J.* **2019**. <https://doi.org/10.1038/s41428-019-0245-9>.
- (22) Choi, H. S.; Liu, W.; Misra, P.; Tanaka, E.; Zimmer, J. P.; Itty, B.; Bawendi, M. G.; Frangioni, J. V. Renal Clearance of Nanoparticles. *Nat. Biotechnol.* **2007**, 25 (10), 1165–1170. <https://doi.org/10.1038/nbt1340>.
- (23) Liu, J.; Yu, M.; Zhou, C.; Zheng, J. Renal Clearable Inorganic Nanoparticles : A New Frontier of Bionanotechnology. *Biochem. Pharmacol.* **2013**, 16 (12), 477–486.

<https://doi.org/10.1016/j.mattod.2013.11.003>.

- (24) Park, J.; Gu, L.; Maltzahn, G. Von; Ruoslahti, E.; Bhatia, S. N.; Sailor, M. J. Biodegradable Luminescent Porous Silicon Nanoparticles for in Vivo Applications. *Nat. Mater.* **2009**, *8*, 331–336. <https://doi.org/10.1038/nmat2398>.
- (25) Handy, R. D.; Shaw, B. J. Toxic Effects of Nanoparticles and Nanomaterials : Implications for Public Health , Risk Assessment and the Public Perception of Nanotechnology. *Health. Risk Soc.* **2007**, *9* (2), 125–144. <https://doi.org/10.1080/13698570701306807>.
- (26) Revell, P. A. The Biological Effects of Nanoparticles. *Nanotechnol. Perceptions* **2006**, *2*, 283–298.
- (27) Liu, K.; Liu, B. Recent Advances in Biodegradable Conducting Polymers and Their Biomedical Applications. *Biomacromolecules* **2018**, *19*, 1783–1803. <https://doi.org/10.1021/acs.biomac.8b00275>.
- (28) Rorije, E.; Germa, F.; Philipp, B.; Schink, B.; Beimborn, D. B. Prediction of Biodegradability from Structure: Imidazoles. *SAR QSAR Environ. Res.* **2002**, *13* (1), 199–204. <https://doi.org/10.1080/10629360290002271>.
- (29) Repenko, T.; Rix, A.; Ludwanowski, S.; Go, D.; Kiessling, F.; Lederle, W.; Kuehne, A. J. C. Bio-Degradable Highly Fluorescent Conjugated Polymer Nanoparticles for Bio-Medical Imaging Applications. *Nat. Commun.* **2017**, *8* (1), 470. <https://doi.org/10.1038/s41467-017-00545-0>.
- (30) Anderson, E. B.; Long, T. E. Imidazole- and Imidazolium-Containing Polymers for Biology

- and Material Science Applications. *Polymer (Guildf)*. **2010**, *51* (12), 2447–2454.
<https://doi.org/10.1016/j.polymer.2010.02.006>.
- (31) Yamamoto, T.; Uemura, T.; Tanimoto, A.; Sasaki, S. Synthesis and Chemical Properties of π -Conjugated Poly(Imidazole-2,5-Diyl)S. *Macromolecules* **2003**, *36* (4), 1047–1053.
<https://doi.org/10.1021/ma0211232>.
- (32) Moncea, O.; Poincot, D.; Fokin, A. A.; Schreiner, P. R. Palladium-Catalyzed C2 \rightarrow H Arylation of Unprotected (N \rightarrow H) -Indoles “ On Water ” Using Primary Diamantyl Phosphine Oxides as a Class of Primary Phosphine Oxide Ligands. *ChemCatChem* **2018**, *10*, 2915–2922. <https://doi.org/10.1002/cctc.201800187>.
- (33) Lombeck, F.; Marx, F.; Strassel, K.; Kunz, S.; Lienert, C.; Komber, H.; Friend, R.; Sommer, M. To Branch or Not to Branch: C–H Selectivity of Thiophene-Based Donor–Acceptor–Donor Monomers in Direct Arylation Polycondensation Exemplified by PCDTBT. *Polym. Chem.* **2017**, *8*, 4738–4745. <https://doi.org/10.1039/c7py00879a>.
- (34) Kuehne, A. J. C.; Gather, M. C.; Sprakel, J. Monodisperse Conjugated Polymer Particles by Suzuki–Miyaura Dispersion Polymerization. *Nat. Commun.* **2012**, *3* (1), 1088.
<https://doi.org/10.1038/ncomms2085>.
- (35) Kawaguchi, S.; Ito, K. Dispersion Polymerization. In *Advances in Polymer Science*; Okubo, M., Ed.; Springer Berlin Heidelberg: Berlin, Heidelberg, 2005; pp 299–328.
<https://doi.org/10.1007/b100118>.
- (36) Peer, D.; Karp, J. M.; Hong, S.; Farokhzad, O. C.; Margalit, R.; Langer, R. Nanocarriers as an Emerging Platform for Cancer Therapy. *Nat. Nanotechnol.* **2007**, *2*, 751–760.

- (37) Beard, P. Biomedical Photoacoustic Imaging. *Interface Focus* **2011**, *1*, 602–631.
- (38) Liu, J.; Wang, S.; Cai, X.; Zhou, S.; Liu, B. Hydrogen Peroxide Degradable Conjugated Polymer Nanoparticles for Fluorescence and Photoacoustic Bimodal Imaging. *Chem. Commun.* **2018**, *54*, 2518. <https://doi.org/10.1039/C7CC09856A>.
- (39) Borek, B. A.; Waelsch, H. THE ENZYMATIC DEGRADATION OF HISTIDINE. *J. Biol. Chem.* **1953**, *205* (1), 459–474. [https://doi.org/https://doi.org/10.1016/S0021-9258\(19\)77270-6](https://doi.org/https://doi.org/10.1016/S0021-9258(19)77270-6).
- (40) Aldawsari, M. F.; Alalaiwe, A.; Khafagy, E.; Saqr, A. Al; Alshahrani, S. M.; Alsulays, B. B.; Alshehri, S.; Lila, A. S. A.; Mohd, S.; Rizvi, D.; et al. Efficacy of SPG-ODN 1826 Nanovehicles in Inducing M1 Phenotype through TLR-9 Activation in Murine Alveolar J774A . 1 Cells : Plausible Nano-Immunotherapy for Lung Carcinoma. *Int. J. Mol. Sci.* **2021**, *22*, 6833.